5-29-2012

Monitoring Photocatalytic Degradation of X-ray Contrast Media with Raman Spectroscopy

Sabina Salkic
Western Kentucky University, Sabina.Salkic@topper.wku.edu

MONITORING PHOTOCATALYTIC DEGRADATION OF X-RAY CONTRAST MEDIA WITH RAMAN SPECTROSCOPY

A Thesis
Presented to
The Faculty of the Department of Chemistry
Western Kentucky University Bowling
Green, Kentucky

In Partial Fulfillment
Of the Requirements for the Degree
Master of Science

By
Sabina Salkic

May 2012

MONITORING PHOTOCATALYTIC DEGRADATION OF X-RAY CONTRAST MEDIA WITH RAMAN SPECTROSCOPY

Date Recommended 5/10/2012

Matthew Nee

Dr. Mathew Nee, Director of Thesis

Jeremy Maddox

Dr. Jeremy Maddox

Eric Conte

Dr. Eric Conte

Rachel C. Doerner 24-May-2012

Dean, Graduate Studies and Research Date

ACKNOWLEDGEMENTS

At first, I would like to thank Dr. Mathew Nee for his thoughtful guidance and support. It is an honor to have you as a research advisor. Besides science, I have also learned the value of mentorship and professionalism from you. Thank you so much for having me in your research group. I would like to thank our research group members for their support: Heather Shockley, Logan Eckler, Brandon Farmer, and Charlotte Homes. Dr. Jeremy B. Maddox for letting us use your server for our calculations. Dr. Bango Yan for letting us use your ultraviolet lamp. My deepest gratitude to my family, especially to my parents, Hajra Salkic and Sadik Salkic, my sisters Suada and Almira, for their unwavering love and enthusiasm. Thanks to Brady Garabato for his help with computational chemistry calculations. Finally want to say thank you to my boyfriend Rasim who supported me throughout this hard work.

TABLE OF CONTENTS

LIST OF TABLES

Table Page

LIST OF FIGURES

MONITORING PHOTOCATALYTIC DEGRADATION OF THE X-RAY CONTRAST MEDIA WITH RAMAN SPECTROSCOPY

Sabina Salkic May 2012 44 Pages

Directed by: Dr. Mathew Nee, Dr. Jeremy Maddox and Dr. Eric Conte

Department of Chemistry Western Kentucky University

X-ray contrast media such as diatrizoate and iohexol have been found in wastewater and drinking water and are difficult to remove because they are resistant to water treatment processes. A removal process can be started with ultraviolet photocatalytic degradation of X-ray contrast media in the presence of titanium dioxide or other catalysts. Raman spectra of diatrizoate and iohexol were taken in an aqueous solution in the presence and absence of titanium dioxide during exposure to ultraviolet radiation. Raman intensity is directly proportional to concentration; therefore, we can measure the rate of the reaction based on changes in the Raman spectrum. Changes were monitored for eight hours. Evidence of photoreaction is observed, indicating that the degradation of X-ray contrast media can be measured using Raman spectra. To our knowledge, this represents the first use of Raman spectroscopy to monitor photocatalytic

degradation in real time, opening a potentially powerful approach to studying the removal of pollutants in the environment.

CHAPTER 1

Photocatalytic Degradation of Pollutants

1.1 Introduction

Recently, increasing attention has been focused on the presence of pharmaceutical compounds in aquatic environments due to their widespread use and incomplete removal during wastewater treatment.[1] For example, iodinated contrast media (ICM), hormones, and other organic compounds are among the most prevalent untreated water contaminants.[2-4] The presence of these pharmaceutical compounds in the environment is a growing concern because relatively little is known about the significance of hospitals as point sources of emission of organic micro-pollutant into the aquatic environment and their impact on human and ecosystem health.[1,3-4]

In recent years, ICM have become the focus of environmental concern as a group of halogenated pharmaceutical compounds. Research studies have identified ICM compounds as the main contributors to the burden of total adsorbable organo-iodine in clinical wastewater.[6] Some ICM have been shown to be unresponsive to compact chemical and biological water treatment processes, which leads to interest in developing more effective and sustainable technologies for treating water sources contaminated with pharmaceutical compounds.[1,5,6]

Estrogenic compounds such as 17β-estradiol and estrone have also been found in treated domestic water effluents. These estrogenic compounds are of great concern because of their potential in altering the normal endocrine function of physiological status

of animals and humans.[7] Much of the research has been motivated by the recent discovery of the role of estradiol in promoting breast cancer.

The objective of this study is to determine if Raman Spectroscopy can be used for monitoring photocatalytic degradation of X-Ray contrast media. We seek to develop a method that is fast (compared to chromatography) and non-invasive, but which still yields results that are consistent with previous studies.

1.2 Iodinated contrast media

Iodinated X-ray contrast media (ICM) are widely used pharmaceutical compounds for the imaging of internal body structure, such as organs, blood vessels, and soft tissues during diagnostic examinations. They are applied at high doses (200 g per application) and are eliminated unmetabolized in the urine within 24 hours.[9] Annual worldwide consumption of ICM is approximately 3.5×10^6 kg.[5] Most of the ICM are classified as ionic or nonionic depending on the functional moieties at their side chains. Scheme 1.1 shows two of iodinated contrast media used in this study. For example, diatrizoate is an ionic ICM: it is negatively charged at neutral pH due to its carboxylate moiety. Nonionic compounds such as iohexol contain functional moieties that are uncharged at neutral pH.[10]

ICM are considered to be safe to humans, but mild acute reactions, such as nausea and pain at the area of injection, have been reported in 15% of patients receiving ionic and 3% of the patients receiving non-ionic ICM.[1] Wastewater treatment processes do not effectively remove ICM resulting in their detection at mg/L levels in effluents of some wastewater treatment plants.[10] Only limited biodegradation of ICM occurs over an

extended period of time (> 20 days), which leads to formation of triiodinated benzoic acid metabolites that are resistant to further transformation. Diatrizoate, in particular, has been found to be less amenable to active sludge biodegradation than other ICM.[11] Compared to other pharmaceuticals, ICM have the highest levels found in environmental samples, which can be as high as micrograms per liter levels.[10] One of the methods used to measure their presence in secondary and tertiary treated wastewater is direct injection-LC/MS/MS. This technique was used to measure eight ICM, which include the two from Scheme 1.1 Amounts detected are found to be 0.11 to 0.97µg/L for ICM in wastewater.[10]

Scheme 1.1: Structures of X-Ray contrast media and estrogens in this study

Diatrizoate

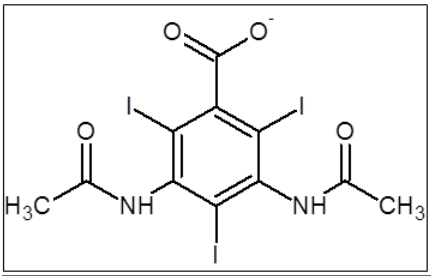

Iohexol

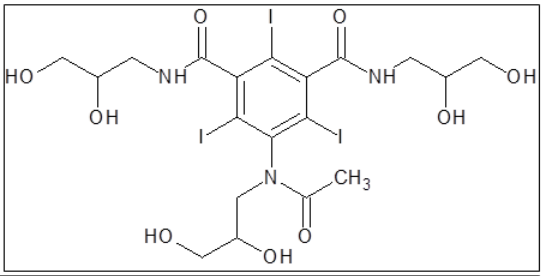

Estrone

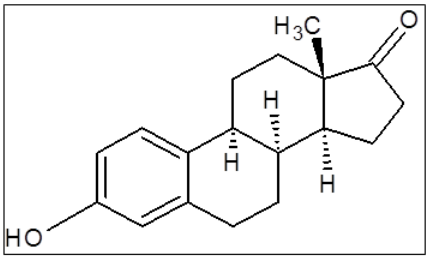

17-β Estradiol

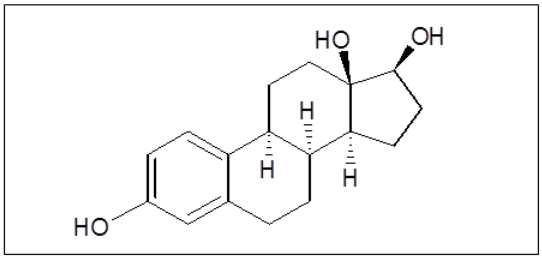

1.3 Estrogens

Other micro-pollutants include steroidal compounds, such as the hormones estrogens and testosterone. These represent a class of compounds generally synthesized from cholesterol. Two estrogens studied here are 17β-estradiol and estrone. As shown in Scheme 1.1, both have molecular structures with a five carbon ring attached to three six carbon rings and hydroxyl group at the same location on the phenyl ring. They are differentiated by the substituent on the pentane ring. Estrogens display characteristics similar to many organic compounds, including low solubility in water and high affinity to organic matter. Estrone has solubility in water of 1.30 mg/L at a pH 7 and a temperature of 25˚C. This is very low, but estrone has been shown to affect the biological systems in concentrations as low as 0.1ng/L.[12]

Estrogens are known to be responsible for the development of secondary sexual characteristics, and to affect growth and function of a wide range of tissues. A number of synthetic agents including pesticides and a variety of other industrial chemicals also have estrogenic activity.[13] Some of the estrogens have been extensively investigated since the role of estradiol in promoting breast cancer was determined.[13-16] Estrogenic steroid hormones have attracted considerable attention, because of enhanced feminization of fish exposed to treated water.[16]According to different studies, human estrogens such as estradiol and estrone are also found in wastewater.[17]

1.4 Direct Removal Techniques

1.4.1 Nanofiltration (NF) and Reverse osmosis (RO)

Although testing for estrogen and ICM in wastewater is a time consuming and expensive process, research and interest in estrogen testing and removal are growing. Because of their low concentrations, chromatographic methods (GC/MS, GC-MS/MS and LC/MS/MS) have typically been used for analysis of estrogens. These methods also work well for testing larger freshwater sources for estrogens.[18] To remove estrogens from wastewater many studies have reported nanofiltration (NF) and reverse osmosis (RO) to be effective methods.[19] Both RO and NF are pressure driven membrane processes that can remove contaminates to 0.001- 0.0001 μm respectively. NF is defined as a process lying between porous ultrafiltration and RO. Both of these processes are used heavily in water and wastewater treatments; RO is also used in desalination. NF only retains multivalent ions, making it a very economical alternative where the retention of monovalent salts is not required.[19] However, for monovalent compounds like ionic ICM, it is not as productive.

1.4.2 Direct contact membrane distillation (DCMD)/ forward osmosis (FO)

Recent studies show direct contact membrane distillation (DCMD) and forward osmosis (FO) are being investigated for wastewater treatment. Membrane distillation (MD) is a separation process in which mass transfer is carried out by evaporation of a volatile solute through a hydrophobic microporous membrane. Benefits of MD are very high rejection of nonvolatile compounds, lower operating pressures than RO and other pressure driven processes, and reduced chemical interaction between the feed solution and the membrane. DCMD is one configuration of MD in which both sides of the membrane are in

contact with aqueous solutions. In DCMD water from the heated feed stream evaporates through the membrane into the cooler permeate stream where it condenses and becomes part of the permeate streams.[20] The FO process results in concentration of a feed stream and dilution of a highly concentrated stream (draw solution-DS).[20] DCMD and FO during investigation shows that the DCMD provides greater than 99.5% hormone rejection and FO provides from 77 to 99% hormone rejection depending on the experiment duration and feed solution chemistry.[20] However, no studies have been done for the removal of ICM from the water by DCMD/FO.

1.5 Advanced oxidation processes

Advanced oxidation processes (AOPs) are reaching popularity in water and waste treatment because of their destructive methods of contaminant degradation. Advanced oxidation processes are characterized by their production of the hydroxyl radical (•OH), a very strong oxidant. AOPs use different reagent systems such as photochemical degradation process (UV/O_3, UV/H_2O_2), photocatalysis (TiO_2/UV) and chemical oxidation processes (O_3, O_3/H_2O_2). The main goal is to produce simple, relatively harmless inorganic molecules, such as CO_2 and H_2O. [21-23] The major advantage of AOPs can be summarized as the complete mineralization of organics and the removal of recalcitrant compounds.

1.5.1 Chemical and Photochemical Degradation

During waste water treatment ICMs were only partially removed by ozonation; about 35 to 55% of non-ionic ICMs and below 20% of ionic ICMs were removed, which shows some success.[21] Here oxidation of ICM does not completely oxidize to CO_2 and

H_2O in many cases. Completion of oxidation reaction can be achieved by supplementing the reaction with the ultraviolet (UV) radiation. This shows that alternative treatment technologies can be developed that would be effective in degrading these compounds. [22-23]

Several studies have focused on removing pharmaceuticals from the environment using UV Disinfection and UV-Oxidation for degradation. UV used for wastewater and drinking water was accomplished using a mercury lamp that emits primarily light at 254nm. UV is widely used for drinking water disinfection in Europe and also in U.S. as well. UV irradiation proved to be effective for decomposing iohexol (X-ray contrast media) with both UV photolysis and UV/H_2O_2 oxidation. During the UV/H_2O_2 oxidation process, elimination of organic compounds may result from direct photolysis following UV irradiation and hydroxyl radical attack. A better ICM removal occurs during treatment with ozone-based advanced oxidation processes that promote •OH formation using UV/O_3 and O_3/H_2O_2 than during O_3 treatment processes where •OH production is not specifically promoted. [24-25]

1.5.2 Photocatalytic Degradation

Another method used for removal of ICM is photocatalytic treatment which was first reported by Honda and Fujishima using titanium dioxide (TiO_2) photo-assisted electrochemical splitting of water in 1972.[26] TiO_2 has found a wide application in the field of environmental treatments. Photocatalytic treatment processes often use semiconductors, such as TiO_2, which has received much attention due to its potential photocatalytic applications in wastewater treatment and air purification. TiO_2 is non-toxic, efficient photo-

catalyst, chemically stable and relatively inexpensive, all important advantages of to support its use.[26-28]

Several studies have looked at development of a catalyst system that is capable of degrading estrogen pollutants in the environment. One of the studies has used a degradation route with a combination of a nitrite and ferric salts as the photocatalyst is for catalytically removing estrogens. After one day of reaction, 86.6 % of the estrogens have been degraded and after 30 days more than 99.9% were removed. The degradation system demonstrates that $FeCl_3/NaNO_2$ is an efficient photocatalyst, which is activated by irradiation with natural light .[21] However, before photocatalysis can become a widely used method, the mechanism and by-products must be well understood. The intermediate oxidation products remaining in the solution may be as toxic as or even more toxic than the initial parent compound.

There are three different forms of TiO_2: anatase, rutile, and brooklite.[31] The difference in catalytic activities is attributed to different crystal lattice structures. The photocatalytic activity of TiO_2 is dependent on surface and structural properties of the semiconductor, such as surface area, particle size distribution, band gap, and surface hydroxyl density.[32] Particle size is important in heterogeneous catalysis because it is directly related to the efficiency of a catalyst through the definition of its specific surface area.[31-32]Because of the wide range of combinations of oxidant and catalysts that can generate $OH\cdot$ radicals, AOPs are widely characterized.

1.5.3 Photocatalysis mechanisms

In the photocatalytic oxidation process pollutants are destroyed with the help of semiconductor photocatalysts, such as TiO_2, a light source, and an oxidizing agent, such as oxygen. The photocatalysis mechanism for the degradation of organic pollutants is shown in Figure 1.1. TiO_2 is only responsive to ultraviolet light (UV) instead of more abundant visible light (bandgap energy E=3.2eV, λ = 387 nm). TiO_2 is a photocatalyst once it is excited by light with energy higher than its band gap. Upon excitation, the electrons in TiO_2 will transfer from the valence band (VB) to an empty conduction band (CB), leading to charge separation and the formation of a strongly oxidizing species.[32-33] Electron (e^-) and electron hole (h^+) pairs will first form on the surface of the photocatalyst. In the presence of O_2 or H_2O, this electron injection will form superoxide (O_2^-) and hydroxyl ($OH^\cdot$) radicals both on the surface and in aqueous solution. Both are highly reactive chemical substances that will oxidize organic compounds into carbon dioxide CO_2 and H_2O.

Photocatalytic oxidation can also be a surface-catalyzed reaction where the target is directly oxidized by h^+. In these cases, a chemical or contaminant must first be adsorbed onto the TiO_2 surface before it can undergo photocatalytic oxidation. The adsorption of substrates on the TiO_2 surface is absolutely necessary for electron or hole processes due to the very fast recombination of electron/hole pairs.[32-34]

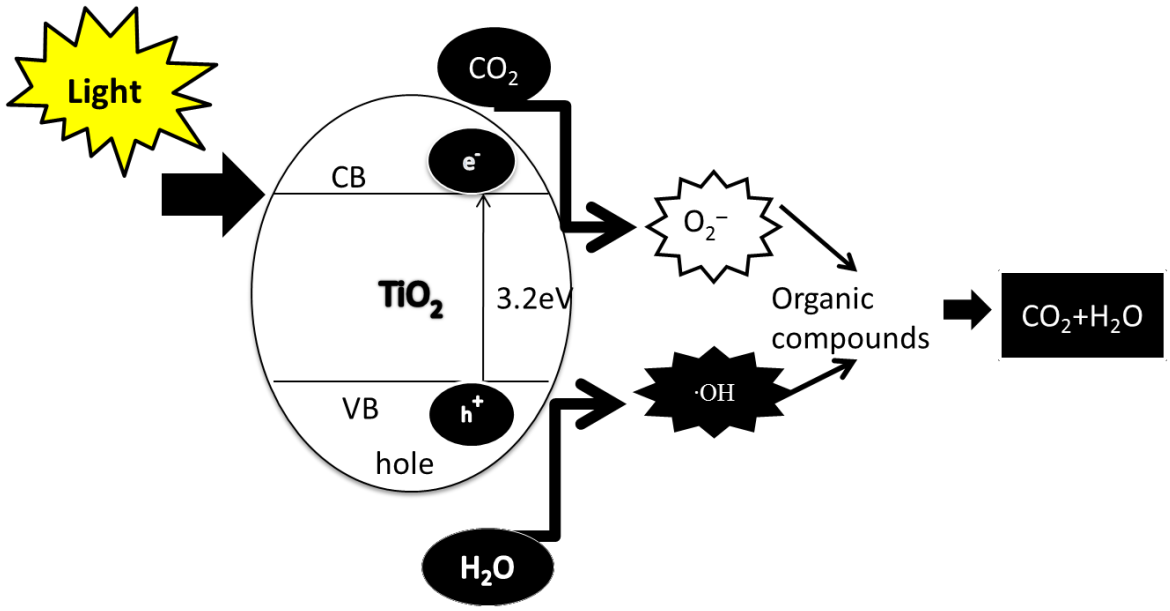

Figure 1.1: Mechanism of photocatalytic degradation. Titanium dioxide (TiO_2) absorbs ultraviolet (UV) radiation from sunlight; it will produce pairs of electrons and holes. The positive hole of titanium dioxide breaks apart the water molecule to form hydroxyl radical. The negative electron reacts with oxygen molecule to form superoxide anion. Hydroxyl radical and superoxide anion react with organic compounds to produce CO_2 and H_2O.

1.6 Overview

Some work has been done on photocatalytic treatment of ICM. Our focus is a removal process that can be started with ultraviolet photocatalytic degradation of diatrizoate and iohexol, in the presence of titanium dioxide or other catalysts. Raman spectra of diatrizoate and iohexol are taken in an aqueous solution in the presence and absence of titanium dioxide during exposure to ultraviolet radiation. Raman intensity is directly proportional to concentration of compounds, therefore we can measure the rate of the reaction based on changes in the Raman spectra. Other studies have used LC/MS to study photocatalytic degradation of ICM. In spite of its sensitivity, the main disadvantage of using chromatographic methods is that during the experiment approximately 30 minutes between samples in needed. Each sample must be extracted from the reaction vessel throughout the degradation process, which is time consuming and there are large chances for sample-to-sample inconsistencies in analysis.

Spectroscopic approaches, such as the ones presented here, can be performed faster and with no sample extraction needed, dramatically increasing the time resolution with which the reactions can be measured. In Chapter 2, the experimental methods used are outlined, with results for photocatalytic studies on ICM presented in Chapter 3. Then, an attempt to improve the sensitivity of our Raman methods using surface-enhanced Raman spectroscopy, extending their application to the estrogens, will be explored briefly in Chapter 4.

CHAPTER 2

Materials and Methods

This chapter outlines in detail the materials and procedures used in this study to accomplish the objectives summarized in Chapter 1. The contaminants selected cover a several common pollutants found in wastewater. Diatrizoate is an ionic compound that has been found to be unresponsive to normal wastewater treatments while iohexol is a non-ionic compound in the same general class (iodinated x-ray contrast media, ICM). Estrone and 17β-estradiol are responsible for the majority of endocrine-disruption in aquatic environments due to their high estrogenic activity.

2.1 Materials and reagents

All chemicals were of reagent grade and used without further purification. Diatrizoate (2, 4, 6- triiodo-3,5-diacetamidoenzoate, sodium salt) and iohexol (5-(N-2,3-Dihydroxypropyl Acetamido)-2,4,6-triiodo-N,N′ bis(2,3dihydroxypropyl) isophthalamide) were purchased from Sigma-Aldrich, St. Louis, MO. Estrone (1,3,5(10)-Estratrien-3-ol-17-one or 3-Hydroxy-1,3,5(10)-estratrien-17-one folliculin) and 17 β-estradiol (1,3,5-Estratriene-3,17β-diol, or 3,17β-Dihydroxy-1,3,5(10)-estratriene dihydrofolliculin) were also purchased from Sigma-Aldrich. The glassware used for the reaction process was a quartz volumetric flask, which transmits ultraviolet light to the solution, whereas fused silica does not. Aqueous solutions were prepared using deionized water (~ 18 MΩ). Photocatalysis experiments were conducted using anatase-form TiO_2 which is also supplied by Sigma-Aldrich. TiO_2, has been used extensively as a model photocatalyst.

2.2 Experimental procedures

1-M solutions of ICM (iohexol and diatrizoate) were made fresh for each experiment using 18 MΩ deionized water. 0.1-M and 0.5-M solutions of ICM were also tried, however they did not show large enough Raman signals for reliable kinetic analysis. 0.5 g TiO_2 (as photocatalyst) was added to each 20 mL sample. Sodium nitrate (0.1 M) was added as an internal standard in the case of the iohexol experiments. We used the nitrate internal standard for iohexol only, but not for diatrizoate. The internal standard must be inert both to reaction and to photo-degradation, it must be water soluble, and must have large enough Raman cross section that it can be detected at low concentrations. Carbon disulfide (CS_2) and carbon tetrachloride (CCl_4) were also explored as internal standards, but their low solubility in water made their detection impossible.

Sample solutions were placed into the apparatus as shown in Figure 2.1. In this apparatus, samples were placed into a quartz round-bottom flask inside the dark chamber, a blackened metal box with one opening in each of two sides. The dark chamber sits on top of a magnetic stir plate; the samples are stirred slowly throughout experiment. A 5-cm diameter opening allows radiation from the Xe-arc lamp (Newport 66902, input power: 50-500W), located to make sure all light strikes on the sample flask. A copper tubular sleeve prevents room light leakage into the dark chamber. On a perpendicular wall of the chamber, the probe of the Raman spectrometer (Raman Systems RS-3000) is kept in place at all times, which reduces sample-to-sample inconsistences. This spectrometer has two different continuous-wave pump lasers (533-nm and 785-nm wavelengths). Data was collected on the unreacted solutions with both wavelengths,

however no differences were observed in Raman spectra. All data presented were collected using 785-nm probe laser. In addition to the Raman spectra of photocatalytic degradation runs collected, data was also collected without photocatalyst and with photocatalyst present, but in the dark.

Ultraviolet light from the Xenon lamp was present for the 8 hours of the experiment of all photocatalytic degradation runs, but was closed during the collection of spectra for about 1 min. We found that both room light and the photocatalytic radiation source interfered with the Raman spectrometer during collection of data. At the beginning of our process for developing the experimental techniques, it became clear that TiO_2 could adhere to the inside surface of the reaction flask even after cleaning. The flask was therefore cleaned with hydrogen peroxide between runs to ensure than no cross contamination occurs.

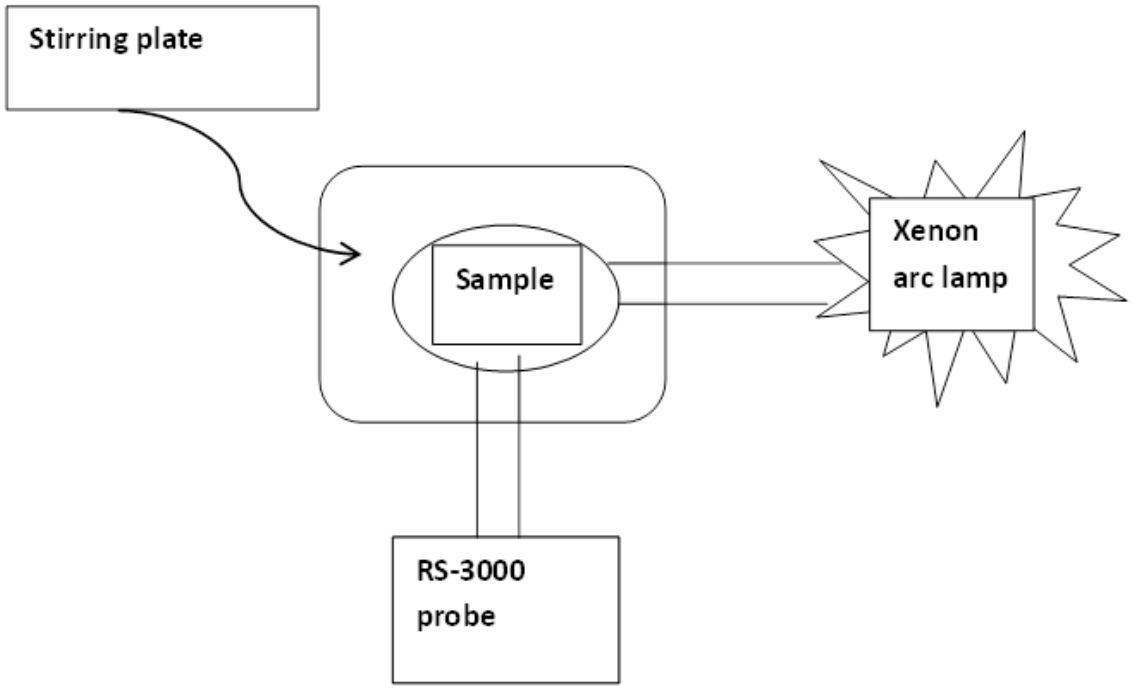

Figure 2.1: Experimental setup with Xenon arc lamp irradiating the sample, which is constantly stirred. The Raman spectrometer is perpendicular of the Xe-lamp. There is a probe aligned to the sample so that spectra can be collected.

2.3 Instrumentation

Many studies have been done to identify the mechanisms and kinetic properties of reaction networks involved in photocatalytic degradation. Chromatographic experiments are commonly used because of their high sensitivity and selectivity. But chromatographic methods do have some limits. During the experiment approximately 30 minutes between samples is needed. Then, each time the sample must be extracted from the reaction flask through the degradation process, filtered, and then preconcentrated, all of which is time consuming. Further, each step presents the risk for sample-to-sample inconsistencies in the analysis.

X-ray contrast media (diatrizoate and iohexol), shown in Scheme 1.1, represent challenges to wastewater treatments. Several studies have shown that diatrizaote can be completely removed using photocatalyst TiO_2. By contrast, previous work has shown that iohexol is photodegraded more successfully in the absence of TiO_2. These X- ray contrast media do have high aqueous solubilities; this is one of the reasons Raman was chosen to monitor photocatalytic degradation. Using Raman does not require a lot of time for sample preparation.

Raman provides us with information about the vibrations of the molecules and covers the same frequency range as infrared (IR) spectroscopy making them complementary. IR spectra are difficult to measure *in situ* where large regions of the spectrum are obscured by water absorption. This means it would not be possible to see much of the ICM because the broad spectrum of water present would obscure the signal from other compounds in the spectrum. Raman and IR also have different selection rules.

Infrared bands arise from an interaction between light and the oscillating dipole moments of vibrating molecules.[36-37]

Raman bands arise from oscillating dipoles caused by light waves interacting with the polarizability of a vibrating molecule. In our case, both ICM compounds are very polar and very polarizable due to the presence of aromatic rings and iodine atoms. Using a probe-type Raman instrument, measurements of the reaction components can be monitored without sample preparation. In our case, sample preparation is only conducted once for each experiment. Another advantage of Raman scattering over infrared absorption is that since it is represented as a shift in frequency from the incident light, it can be acheived with visible light, for which it is possible to create detectors with much higher efficiencies than infrared radiation. It is predominantly applicable to the qualitative and quantitative analyses of covalently bonded molecules.

A Raman spectrometer consists of four components: a laser source, a sample-illumination system and spectrometer (wavelength sector) with a detector. A sample is normally illuminated with a laser beam in the ultraviolet, visible or near infrared range. Scattered light is collected with a lens and is sent through a spectrometer to obtain Raman spectrum of a sample. An important note about Raman scattering is that it does not involve the absorption of the photon, or the emission of a photon of less energy, which instead describes florescence. The difference between Raman scattering and fluorescence is that in Raman scattering, the incident photon is not fully absorbed but rather perturbs the molecule, exciting or de-exciting vibrational or rotational energy states. In fluorescence, the photon is completely absorbed which promotes the molecule to a higher electronic state, and then the emitted photon is due to the molecule's decay back to a

lower energy state.[36-37] Thus, Raman is far less likely to contribute to the photochemistry of the system under study than fluorescence methods.

2.4 Computational Chemistry

For ICM, (diatrizoate and iohexol) quantum computational chemistry was used to compare our experimental results with calculated values of vibrational modes. All calculations were conducted using the GAUSSIAN 09 software package.[40] Electronic structure calculations (optimized geometries and frequency analysis) were performed using the Becker, three-parameter, Lee-Yang-Parr (B3LYP) density functional with the Los Alamos National Laboratory 2 Double-Zeta (lanl2dz) basis set. This basis set is widely used to model heavy atoms (those with many electrons).

Geometry optimization was calculated by B3LYP/lanl2dz to find the configuration of minimum energy of the molecule. To calculate the geometry the program determines the energy at a starting geometry and begins to search for a new geometry of a lower energy. [39]In our study for diatrizoate and iohexol we found that B3LYP/lanl2dz took less time than B3LYP/3-21G, which was also attempted initially. This is why we chose B3LYP/lanl2dz to calculate vibrational frequency for both iohexol and diatrizoate. In each case, the Raman intensities were calculated for all vibrational modes.

CHAPTER 3

Photocatalytic degradation of diatrizoate and iohexol

The photocatalytic oxidation of a wide variety of organic compounds in aqueous solutions has been reported.[41] Irradiation of suspended TiO_2 powder leads to the separation of electrons and holes. Both electrons and holes can react with organic pollutants adsorbed on to the surface of TiO_2 particles. Under favorable conditions, organic matter adsorbed onto the surface of the photocatalyst can be directly oxidized by electron transfer to combine with the hole. Hydroxyl radicals are powerful oxidants which are able to oxidize many substrates even away from the TiO_2.[41-43] While electrons may reduce adsorbed oxygen to O_2^-, the hole can oxidize absorbed water or hydroxide ions to OH· radicals.

Raman spectra of 1-M solutions of diatrizoate and iohexol before it was exposed to irradiation are shown in Figure 3.1. Structures for each target molecule are shown in the inset. In each case, multiple peaks are observed throughout the spectrum, each corresponding to different vibrational modes. To help interpret the Raman spectra, calculations were done on iohexol and diatrizoate as shown in Table 3.1. Here we assign peaks of experimental to calculated frequencies for both of iohexol and diatrizoate. Although most molecular motions were delocalized its own molecule, many could be described based on a single functional group motion. We then assign vibrational mode based on assigned peaks for experimental peaks. Most of the modes correspond to an aromatic ring vibrational mode according to our calculations presented in Table 3.1.

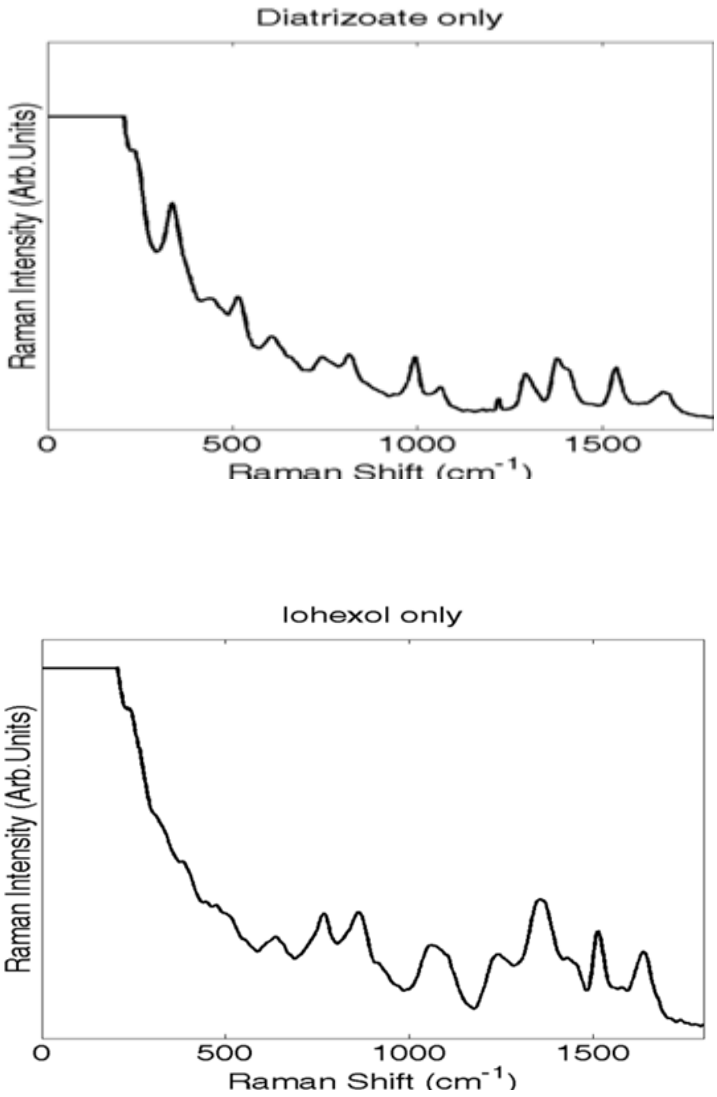

Figure 3.1. Raman spectra of aqueous 1-M solutions of diatrizoate and iohexol. Structures are shown in the insert. In each case, multiple peaks are seen in the spectrum, nearly all of which correspond to aromatic ring vibrational modes.

Table 3.1: Calculation results of the vibrational frequencies of diatrizoate and iohexol. Calculations were done using B3LYP density functional with the LANL2DZ basis set.

Diatrizoate

Experimental Wavenumber (cm^{-1})	Calculated Wavenumber (cm^{-1})	Raman activity	Vibrational Mode
602.2	592.91	9.08	C_6H_6- rocking
742.7	676.92	15.86	C_6H_6- rocking CO_2-bending
820.2	866.58	13.32	C_6H_6- rocking
993.1	988.79	27.94	C_6H_6- bending
1064.0	1102.68	24.59	C_6H_6- wagging
1295.4	1300.37	16.65	C_6H_6- rocking
1379.3	1341.35	85.49	C_6H_6-wagging
1540.2	1480.86	187.91	C_6H_6 - breathing

Iohexol

Experimental Wavenumber (cm^{-1})	Calculated Wavenumber (cm^{-1})	Raman activity	Vibrational Mode
640.3	758.11	8.2	C_6H_6-wagging
766.2	768.25	8.62	C_6H_6-breathing
860.4	881.31	36.75	CH_2-rocking
1059.2	1081.73	20.19	C_6H_6-breathing
1235.3	1285.86	18.01	C_6H_6- breathing
1354.4	1385.31	22.08	C_6H_6-wagging
1511.3	1540.78	17.78	OH-bending CH_2-bending
1633.2	1595.3	19.21	C_6H_6-rocking

3.1 Diatrizoate

One study recently reported on the oxidation of diatrizoate. A series of reaction products detected by LC-ESI (-)-MS/MS suggest that ipso attack of OH· at iodo sites on the aromatic ring lead to hydroxide substitution and iodide release as shown in Scheme 3.1.[44]

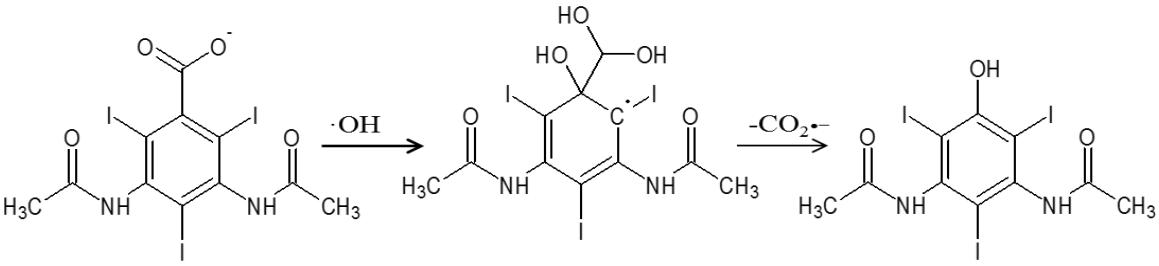

Scheme 3.1 Proposed mechanisms (Jeong) of hydroxyl radical attack on iodo substituent.

Structural assignments made in Scheme 3.1 were confirmed by mass spectral fragmentation patterns, based on data that could not be collected faster than every 30 minutes. Figure 3.2 shows Raman spectra throughout the photocatalytic degradation of diatrizoate with absence of TiO_2 suspensions. In this case, multiple peaks are observed in panel (a) through the spectrum. Panel (b) shows integrated peak area of the spectra of Figure 3.2(a) as function of time. Peak areas were determined by first determining a set of center frequencies. For each center frequency, the peak was fit to a Gaussian peak shape using the PEAKFIT algorithm in the MATLAB software package. In the event that more than two peaks did not appear resolved, multiple peaks could be fit using this algorithm. As a result of using peak fitting software, the areas of the peaks are independent of fluctuations in the baseline. However, total signal fluctuations between sample times are not accounted for in the diatrizoate data.

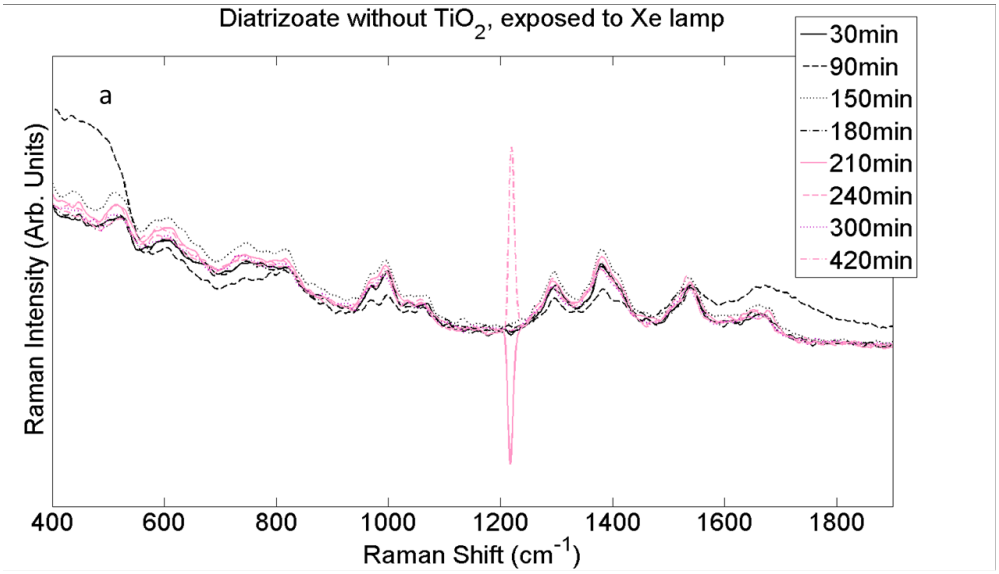

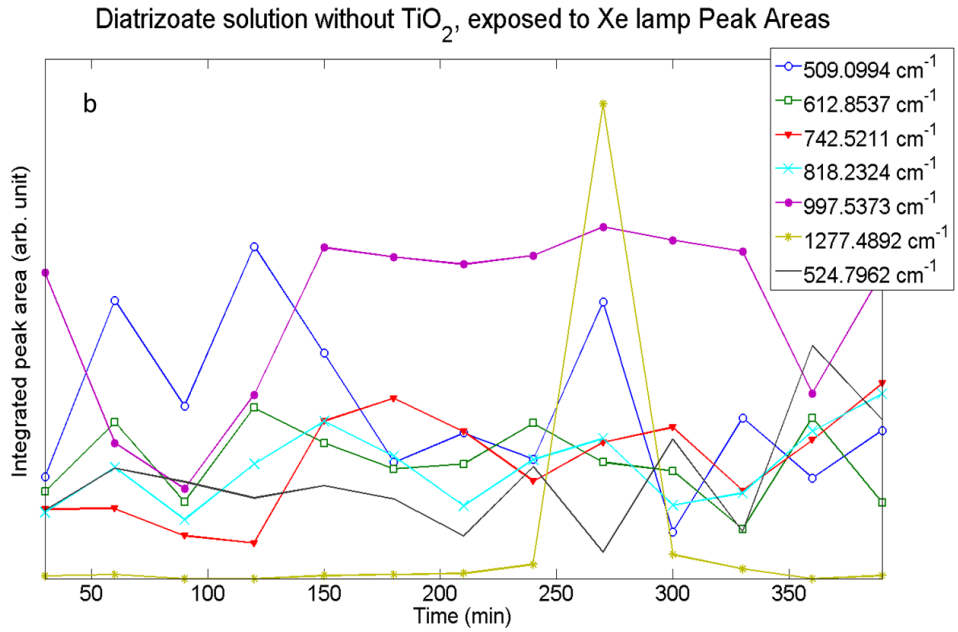

Figure 3.2: Raman spectra (a) during photocatalytic degradation experiments for diatrizoate without TiO_2 photocatalyst. Integrated areas (b) of peaks in the spectra as a function of time.

All peaks monitored remained effectively constant in total area for 8 hours. This is not surprising: previous reports of solar direct photolysis of iodinated X-ray contrast media, have reported only a small fraction of diatrizoate is degraded by UV irradiation in the absence of TiO_2.[43]

Figure 3.3 shows degradation of diatrizoate in the presence of TiO_2 suspensions during irradiation. To account for fluctuations between sample times, each peak is normalized to a relatively stable, low frequency peak (521 cm^{-1}). The overall decrease in all peaks in the Raman spectrum with time indicates degradation of compound, compared to the generally constant peak areas in the absence of the photocatalyst. Some of the changes in the spectrum are observed in the 620 cm^{-1} peak, which is assigned to the carboxylate moiety circled in the structure shown in the inset of Figure 3.3. Changes in the spectral lines shape of the 620 cm^{-1} peak indicate that this peak changes frequency slightly during the course of the experiment. This is consistent with the previously reported loss of COO^- as an early step, as shown in Scheme 3.1 [44] In that scheme, addition of OH radical at the ring reduces the neighboring carbonyl group to a hydroxyl group. This would be expected to alter the COO^- bending frequency, all of which is consistent with both our data and our calculations. Figure 3.3(b) also shows integrated peak areas of the spectra of Fig. 5(a) as function of time to display changes of each peak as function of time. The broad peak centered around 1500 cm^{-1} may indicate TiO_2.

In further support of this, the Raman spectrum of TiO_2 suspended in water is shown in Figure 3.4. It remains unclear why the photocatalyst component is occasionally seen to be very large, though surface enhancement is one possibility. Because the mixture is constantly stirred, surface

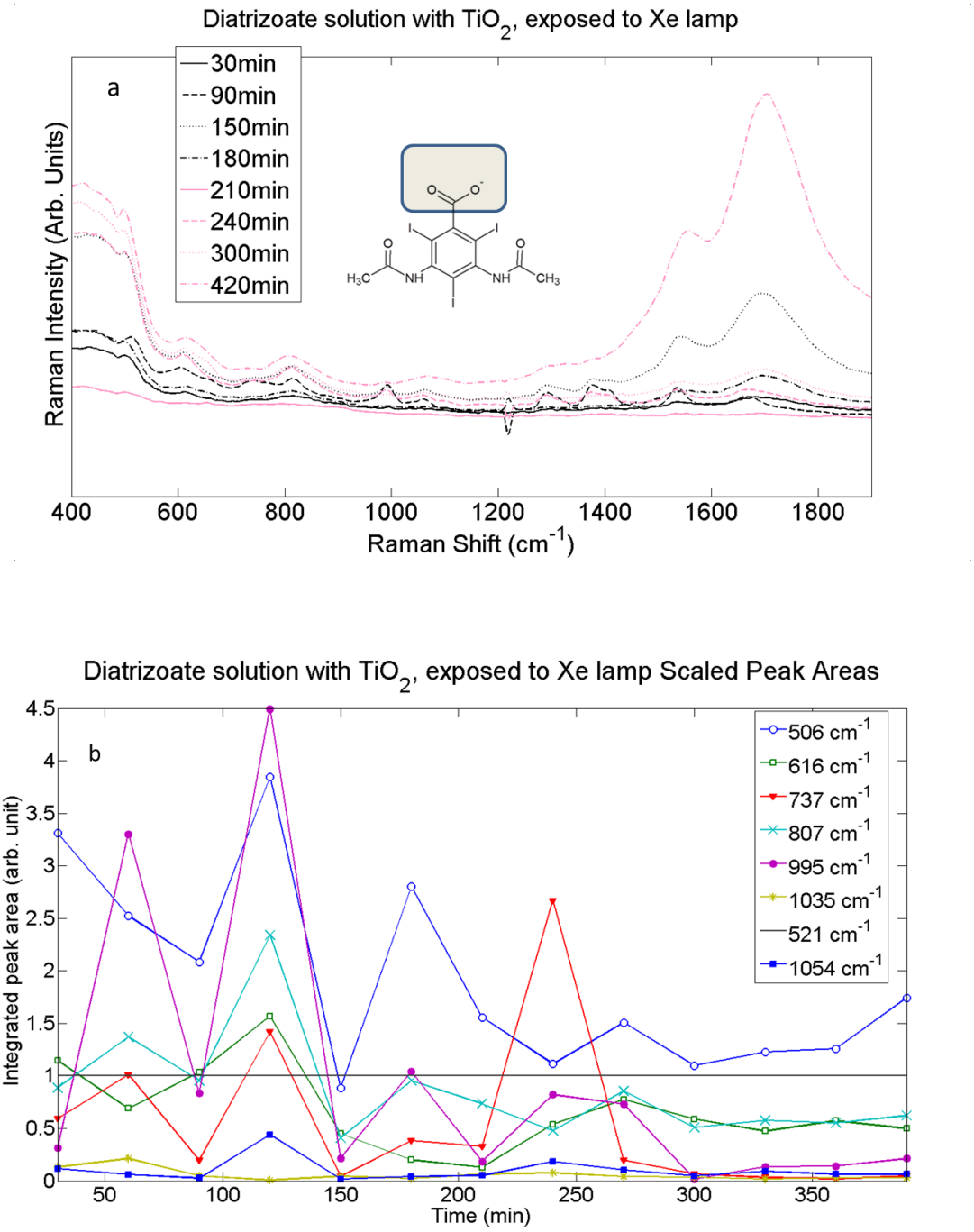

Figure 3.3: Raman spectra (a) during photocatalytic degradation experiments of diatrizoate with TiO_2. Areas of peaks (b) in the spectra as function of time. Decrease in all peaks in Raman with time indicates degradation of compound.

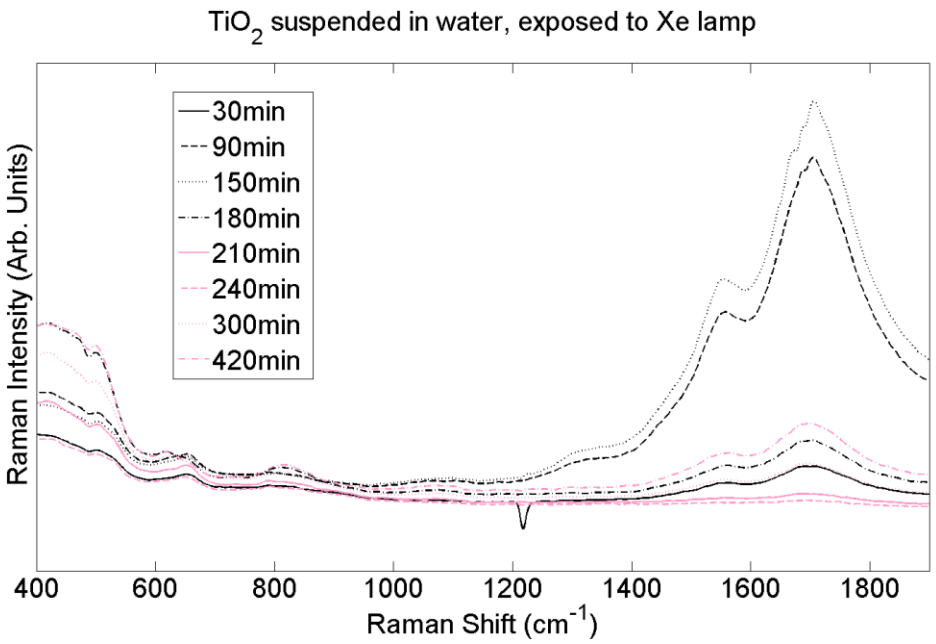

Figure 3.4: Raman spectra of titanium dioxide (TiO_2). Where most of the time peaks reminds constant, except at 1.5 hours a peak appears than dissipates over the next 2.30 hours.

enhanced Raman effects could occur only when a titanium dioxide particle is momentarily in the focus of the pump laser. Consistent with other studies, degradation of diatrizoate occurs faster with TiO_2 than without TiO_2. However, previous studies show that more than 95% of diatrizoate with TiO_2 is degraded with in the first hour.[43] At best here we see only 50% degradation in eight hours. To make our results better we may try other photocatalysts or even adjusting the reaction pH, as previous studies used a pH of 9.

3.2 Iohexol

Previous studies have reported the formation of the first intermediate of iohexol photodegradation by oxidation of the primary alcohol groups. It appears that the primary hyrdoxylate moieties are oxidized first, as indicated in Scheme 3.2. This initial oxidation is followed by decarboxylation and cleavage of N-C bond (deactylation and removal of hydroxylated propanoic acids). Oxidation of the carbon atom attached to the nitrogen is

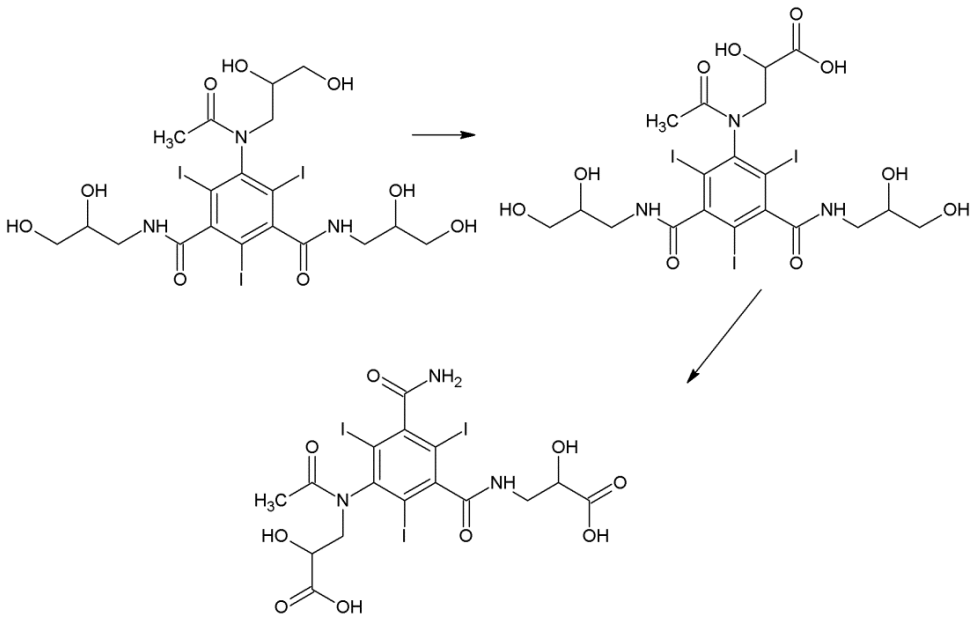

Scheme 3.2: Proposed mechanisms for iohexol degradation.[46]

necessary to promote the cleavage at the N-C bond. It remains unclear, however, whether decarboxylation and oxidation of the hydroxyl group were required prior to cleavage of the N-C bond or if direct cleavage of the N-C bond could occur. [43, 46] Other authors indicate that iohexol degrades only in the *absence* of TiO_2.[48]

Figure 3.5(a) shows Raman spectra of aqueous 1-M iohexol solutions exposed to ultraviolet radiation, without any TiO_2 suspension. Compared to diatrizoate, fewer peaks are observed in the spectrum. The large peak centered around 1000 cm^{-1} is due to the addition of 0.1M sodium nitrate as an internal standard. The peak around 1200 cm^{-1} is a bad pixel in our detector; this is not sample dependent. Figure 3.5(b) shows integrated peak area as a function of time (scaled by the internal standard), monitoring changes of each peak over time. By dividing the peak area of each peak in the spectrum by the internal standard, we are able to better account for signal fluctuations that might occur due to laser power changes or local inhomogeneities. The decrease in all peaks in Raman with time indicates degradation of the compound. This is consistent with previous results, but different from that shown for diatrizoate, which does not show photodegradation in the absence of photocatalyst.

There are striking peak changes around 1540cm^{-1} shown in the Figure 3.6, which show three peaks around 1540 cm^{-1}. Minor changes occurred for the highest peak. However for the peak at1515 cm^{-1} it shows when this peaks was decreasing, the peak around 1490 cm^{-1} starts increasing .The calculations in Table 3.1 indicate that this peak is due to either the OH or CH_2 groups, as circled in the inset of Figure 3.5. Although we are unable to assign the two peaks unambiguously based on the calculations, both of these functional groups have been implicated by previous studies as sites of early attacks in the

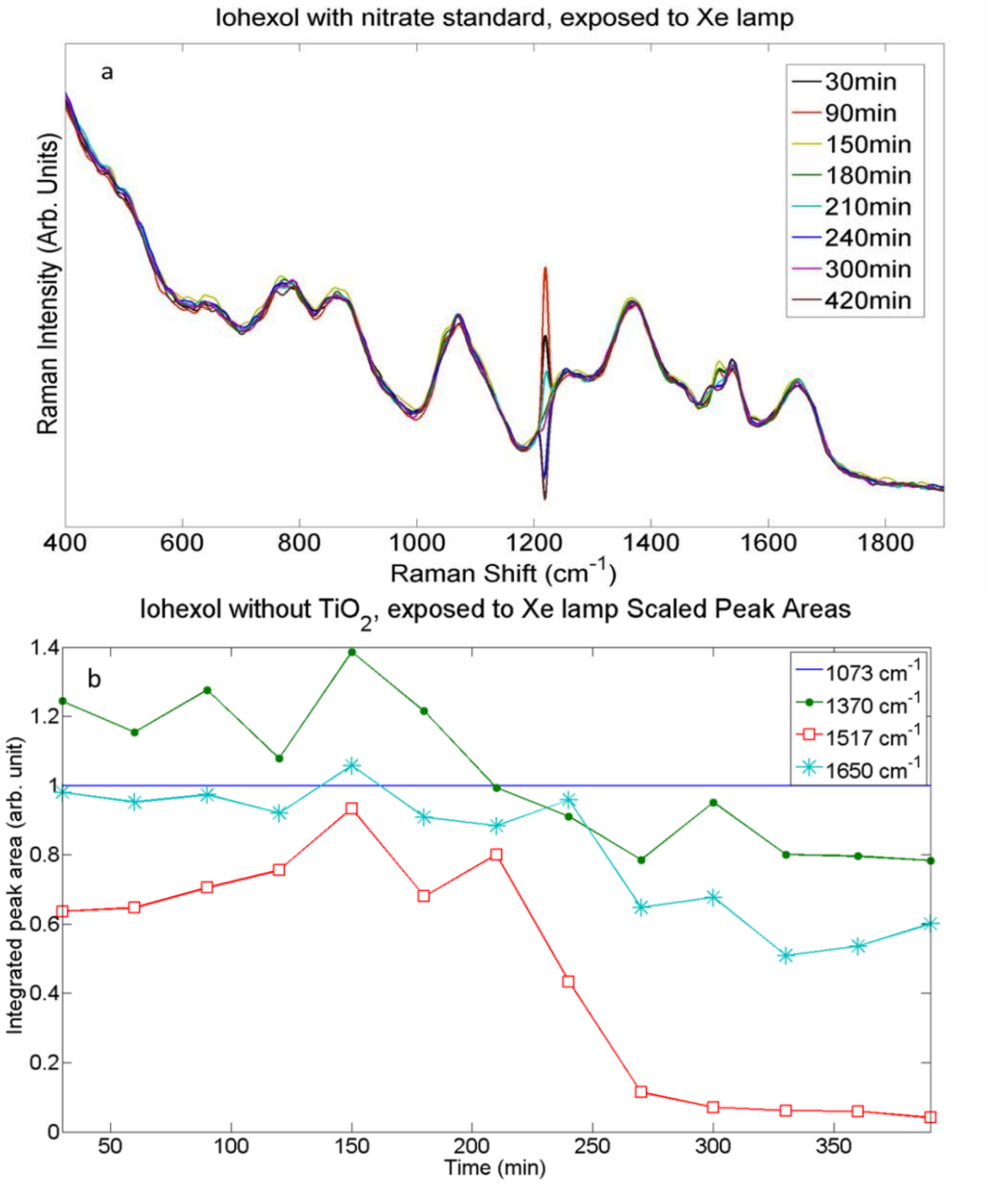

Figure 3.5. Raman spectra of iohexol (a) in the presence of UV radiation without TiO_2 photocatalyst.1540 cm^{-1} vibrational mode changes indicates initial attack at either the OH or CH_2 groups. Areas of peaks (b) in the spectra as a function of time show a decrease in all peaks in Raman with time, indicating degradation of parent compound.

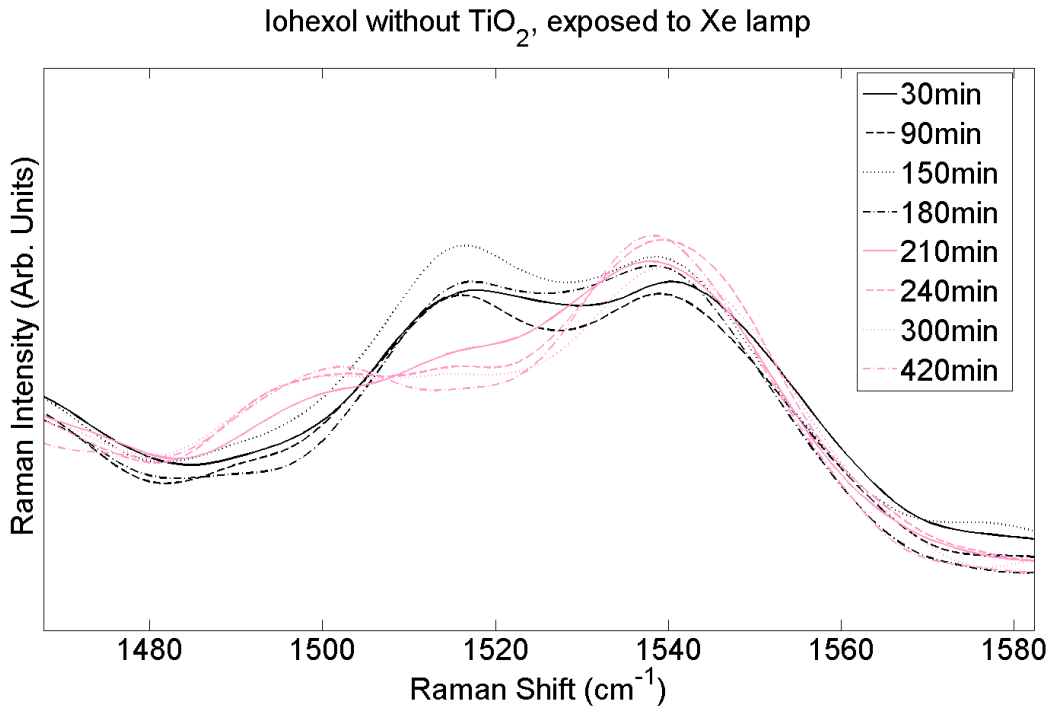

Figure 3.6. Raman spectra of Iohehxol where we zoom in peak that's around 1540cm^{-1} vibrational mode changes indicates initial attack at either the OH or CH_2.

UV degradation process (as indicated in Scheme 3.2).[46]

In Figure 3.7 the Raman spectrum of Iohexol with TiO_2 during photodegradation is shown. By comparing the same peaks as in Figure 3.5, we see an overall degradation of the parent compound. Both qualitatively and quantitatively, the degradation process appears to be unchanged by the presence of photocatalyst. Thus, the decrease in all peaks in Raman with time indicates for both iohexol only and ionexol with TiO_2 degradation of compound. This is not the same as has been reported previously, which indicated that no degradation could be observed in the presence of the photocatalyst. Previous work did not offer any explanation about mechanisms of inhibition.

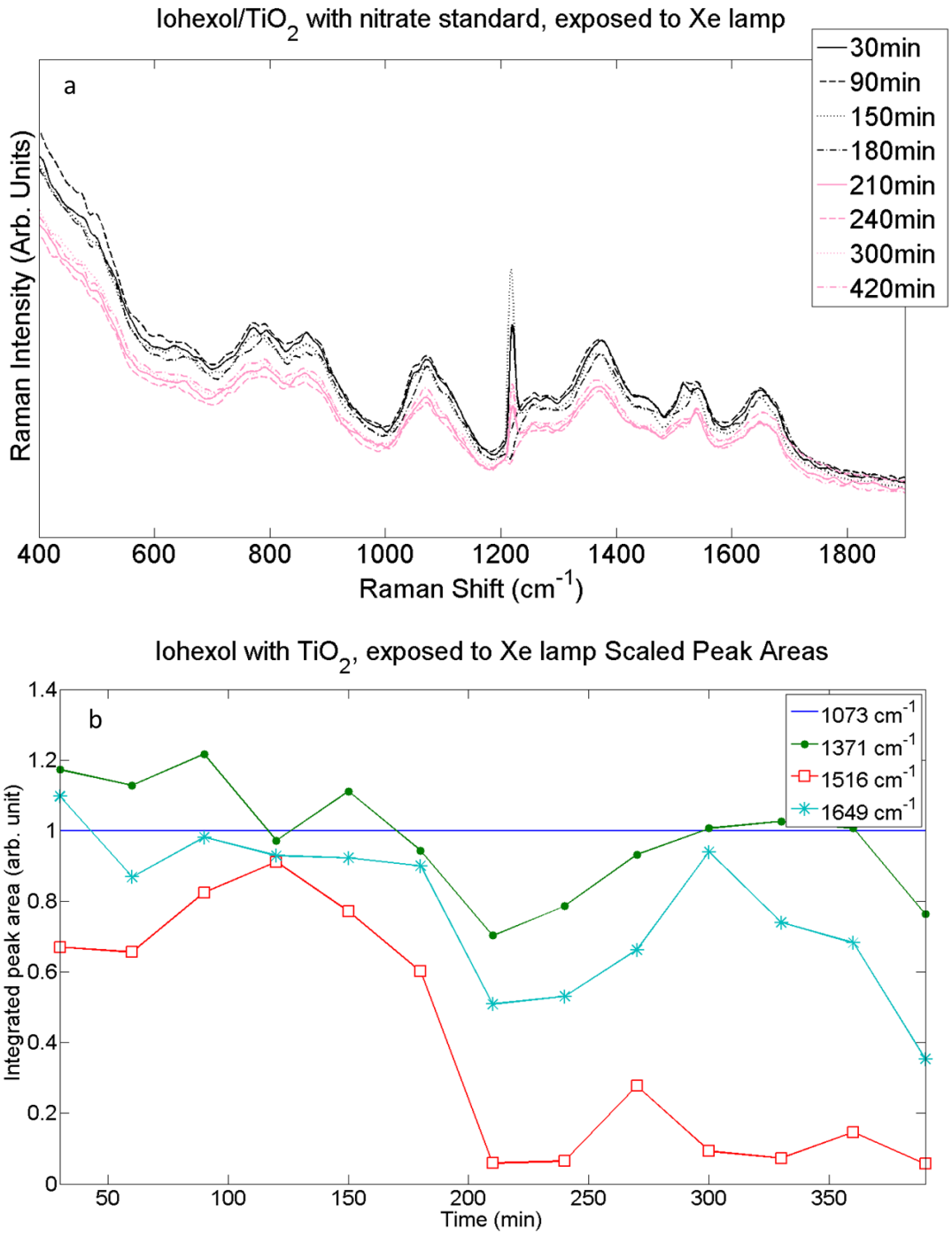

Figure 3.7. Raman spectra of iohexol (a) in the presence of UV radiation with TiO_2 photocatalyst. 1540 cm^{-1} vibrational mode changes indicates initial attack at either the OH or CH_2 groups. Areas of peaks (b) in the spectra as a function of time show a similar decrease in all peaks to that seen in the absence of the photocatalyst.

CHAPTER 4

Surface Enhancement Raman Spectroscopy for Analysis of Estrogen Degradation

The presence of estrogens, a class of endocrine disrupting compounds, in water has caused increasing concerns over their adverse impacts on environmental health. Estrogens display characteristics similar to many organic compounds, including low solubility and a high affinity to organic matter. Some of the most important and commonly found estrogen hormones include estrone and 17β-estradiol. In this study our goal was to monitor photocatalytic degradation of two natural estrogens (17β-estradiol and estrone) with Raman Spectroscopy, as was conducted with X-ray contrast media. However, estrone has solubility in water of 1.30 mg/L at pH 7 and a temperature of 25˚C.[49] 17β-estradiol is also insoluble in water.[49] Because of these low solubilities and weak Raman cross sections of estrogens, surface enhanced Raman spectroscopy (SERS) was investigated to make estrogen spectra easier to monitor.

Surface-enhanced Raman Scattering was conceived in the mid-1970s. The first measurement of a surface Raman spectrum from pyridine adsorbed on an electrochemically roughened silver electrode was reported by Fleischmann,Hendra, and McQuillan in 1974 which stemmed from their pioneering work on applying Raman spectroscopy to the *in situ* study of electrode surfaces.[50]

This technique provides greatly enhanced Raman signal for Raman active molecules that have been adsorbed on certain specially-prepared metal surfaces. The major contribution to the intense Raman signal is due to an enhancement of $10-10^7$ times compared to the intensities predicted from the scattering cross sections of the chosen

compound. The importance of SERS is both that surfaces can be selective but also highly sensitive, whereas traditional Raman spectroscopy is neither. Selectivity of surface signal results from the presence of the surface enhancement (SE) mechanisms only at the surface. The surface signal overwhelms the bulk signal, making bulk subtraction unnecessary.[51-52]

There are two aspects to enhancement: electromagnetic and chemical enhancement. The majority of the overall SERS enhancements is due to electromagnetic enhancement mechanism, which depends on the presence of the metal surface roughness features. The chemical enhancement explains why the analyte molecule adsorbs onto the surface and interacts with the surface chemically. Large enhancements are observed from silver, gold, copper and sodium metal surfaces.[53]

One of the studies have been done to examine the optical enhancement of differently sized silver particles on the SERS spectra of Rhodamine 6G. Atomic Force Microscopy is used to determine the size of the particles which are responsible for the analyses' signal enhancement. Silver particles are responsive to three excitation wavelengths: 488nm, 568nm, and 647nm.[54]

In our case we used gold nanoparticles as our metal surface, which are prepared by Dr. Dakshinamurthy's research group. They have published a synthetic approach for the production of gold nanoparticles (GNPs) that uses biomolecules as both reducing and capping agents.[3] The shape of the particles are spherical, monodisperse, and can be selectively produced within a specific plasmon absorption range by adjustment of synthetic parameters. GNPs were syntehesized by the reduction of Au^{3+} ions in an

aqueous dextrose solution dispersed from a medium pH ~ 6.9. Preparation of an aqueous stock solution of $KAuCl_4$ or $HAuCl_4$ was added to the aqueous medium, containing different concentrations of the dextrose. Samples were places in an orbital shaker with a stirring speed of 150 rpm at room temperature for about 6 hours.[55]

The upper panel of Figure 4.1 shows the Raman spectrum of the GNP untreated with an estrogen. Although some broad features are observed around 700 cm^{-1} and 1700 cm^{-1}, overall the spectra are relatively featureless. The lower panel shows the powder spectrum of estrone. A broad feature near 1500 cm^{-1} is also present. Following a procedure crashed designed to bond the estrogens to the surface of the nanoparticles the spectrum shown in the middle panel of Figure 4.1 is seen. There were no significant changes to the solution phase spectra that would indicate SERS had been accomplished. However, when the nanoparticles are salted out of solution with NaCl, three peaks are obsrved that match the powder spactrum of estrone. These peaks appear at 600 cm^{-1}, 800 cm^{-1} and 1300 cm^{-1}.

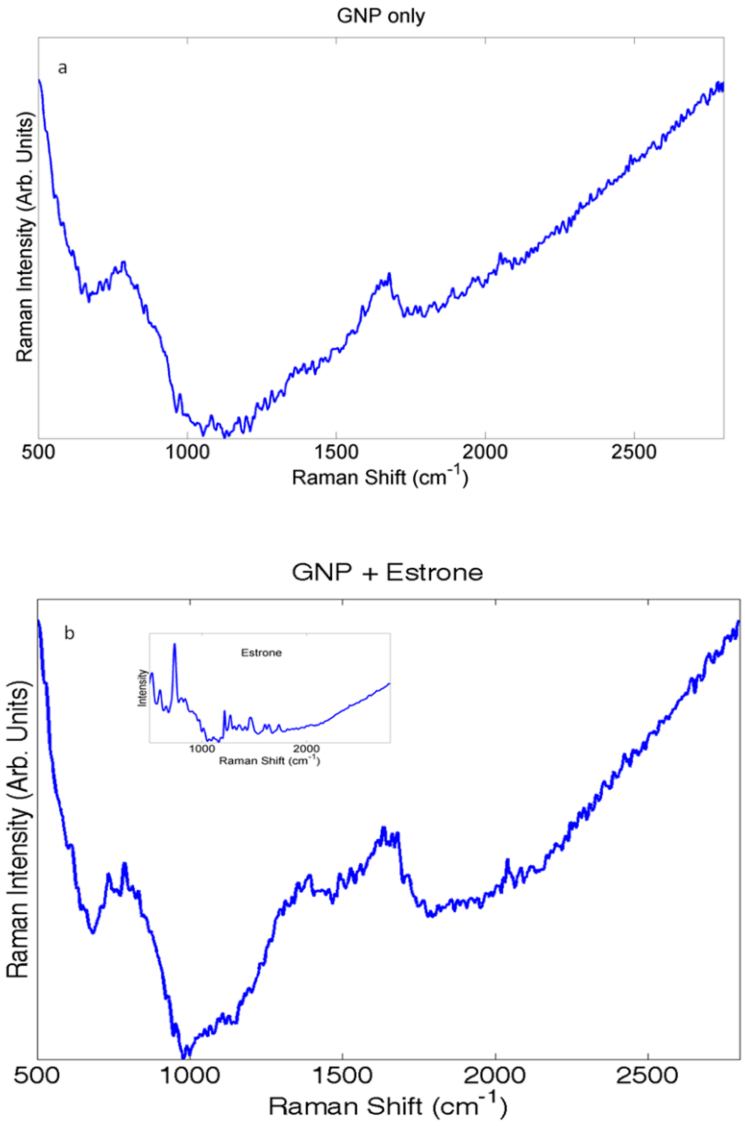

Figure 4.1. Raman spectra of estrone enhanced by surface plasmon resonance: (a) the spectrum of the GNP substrate; (b) shows the Raman spectra collected when estrone is functionalized onto the nanoparticles. A powder Raman spectrum is shown in the inset.

The spectra of aggregated estrone-functionalized GNPs were collected using a pump wavelength of 785 nm, even though the plasmon is resonant at 530 nm. Spectra collected at 532 nm showed significant fluorescence and were not useful for Raman spectra. The surface-enhancements of the Raman signal are significant even at 785nm, consistent with work by others. Figure 4.2 shows the powder Raman spectra of 17-β-estradiol as an insert. No evidence of the estrogen spectrum is seen even in saturated aquaeous of 17-β-estradiol.When it is crashed with NaCl no different peaks where present that are in powder spectra of 17-β-estradiol.

Even though this technique provides great enhancement of the Raman signal for Raman active molecules that have been adsorbed on certain specially prepared metal surfaces, in our case, where we want to monitor photocatalytic degradation of estrogens would not work. According to the Raman spectra of estrone there is a some evidence that it may work, but only when the particles are salted out. However for 17-β-estradiol has not shown an inication that it would work even when we the GNPs are aggregated by salting out. Since the time of these experiments, the market has been flooded with commercially available SERS substrates, which may offer a simple alternative to our experiments here.

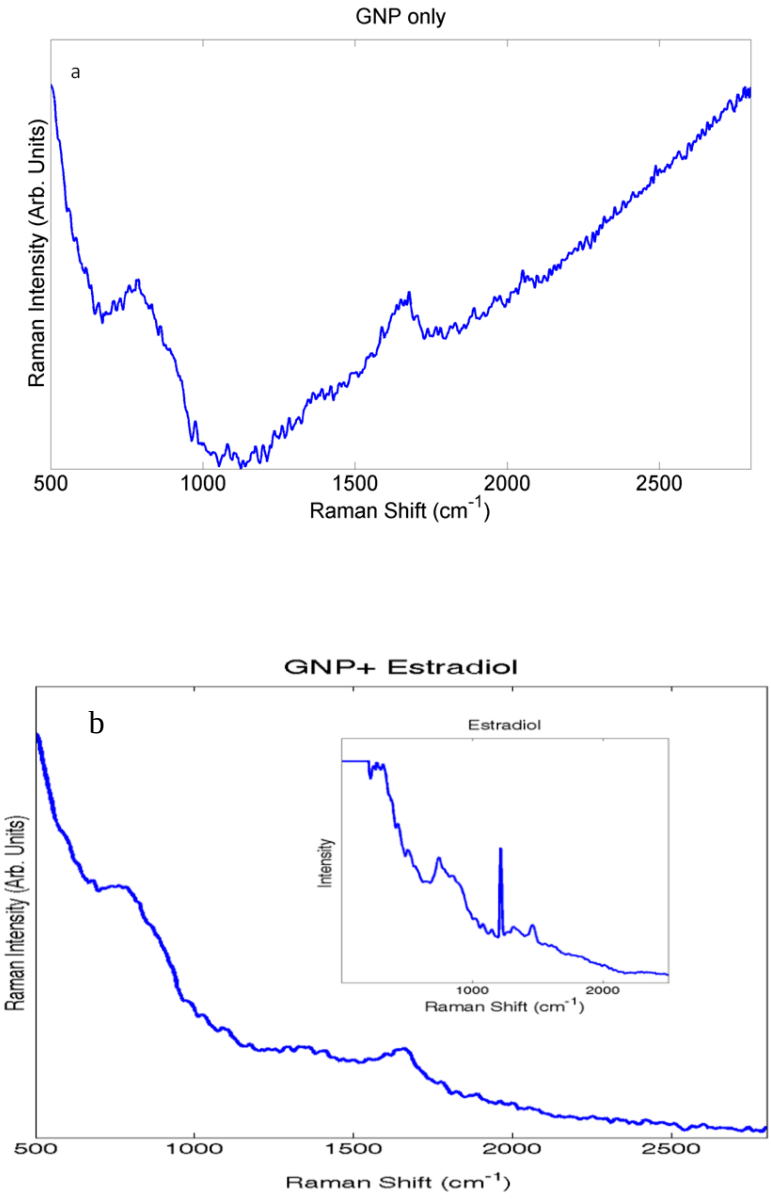

Figure 4.2: Raman spectra of 17β-estradiol enhanced by surface plasmon resonance a) Shows the spectrum of the GNP substrate, b) while shows the Raman spectra collected when 17β-estradiol is functionalized onto the nanoparticles. A powder Raman spectrum is shown in the inset.

CHAPTER 5

Conclusion and Future Research

This thesis focused on developing a method for monitoring photocatalytic degradation kinetics and mechanisms that is fast (compared to chromatography) and non-invasive, but which still yields results which are consistent with previous studies of photocatalytic degradation of X-ray contrast media (ICM). Previous studies have used GC/MS and LC/MS to study photocatalytic degradation of ICM. The main disadvantage of using chromatography methods is that during the experiment approximately 30 minutes between samples is needed. Each sample must be extracted from the reaction vessel throughout the degradation process, which is time consuming and there are large chances for sample-to-sample inconsistencies in analysis.

Our focus was a removal process that can be started with ultraviolet photocatalytic degradation of diatrizoate and iohexol, in the presence of titanium dioxide or other catalysts. The new method that we have developed uses Raman spectroscopy to monitor photocatalytic degradation of ICM. This approach can be performed faster and with no sample extraction needed, dramatically increasing the time resolution with which the reactions can be measured. Results for diatrizoate exposed to ultraviolet light show all peaks monitored remain effectively consistent through experiment. Diatrizoate in the presence of TiO_2 exposed to ultraviolet light showed a change in the spectral lines shape at 620 cm^{-1}, indicating attack at the carboxyl site observed as function of time. All peaks in the Raman spectra decrease with time indicating degradation of compound. Results for Iohexol exposed to ultraviolet light shows peak frequency changes for the 1540 cm^{-1}

vibrational mode. These changes indicate initial attack at either the OH or CH_2 groups on the side chains off of the aromatic ring. Iohexol with TiO_2 shows all Raman peaks decrease with time, indicating degradation of the compound. Our results are consistent with previous studies, meaning Raman can be used to monitor photocatalytic degradation of ICM. To our knowledge, this is the first time photocatalytic degradation has been monitored *in situ* spectroscopically, with the potential for real time measurements.

Throughout the experiment we measured the kinetics every 30 minutes. In the future we can monitor changes using five minutes intervals. Soon, we will compare Raman and LC/MS simultaneously to identify intermediates that are forming throughout the degradation process. We will also study different X-ray contrast agents or other organic pollutants in aquatic environments due to their widespread use and incomplete removal during wastewater treatment.

We also attempted to monitor photocatalytic degradation with two natural estrogens. Because of their low solubility and weak Raman cross sections of estrogens, surface enhanced Raman spectroscopy (SERS) was attempted to make estrogen spectra easier to monitor. However our attempt to improve the sensitivity of our Raman methods using surface-enhanced Raman spectroscopy was not as successful as we would like to be. New methods need to be developed in the future to study photocatalytic degradation of estrogens or other trace compounds.

BIBLIOGRAPHY

1. Jeong, J.; Jung, J.; Cooper, J. W.; and Song. W. *Water Res*. **2010**, 4391-4398.

2. Kormas, L. J.; Schulz, M.; and Ternes A. T. *Environ. Sci. Technol*. **2011**, 45, 8723-8732.

3. Schulz, M.; Loffler, M. W.; and Ternes A. T. *Environ. Sci. Technol*. **2008**, 42, 7207- 7217.

4. Kolpin, W. D.; Furlong, T. E.; Meyer, T. M.; and Thurman, M. E. *Environ. Sci. Technol.* **2002**, 36, 1202- 1211.

5. Perez, S.; and Barcelo, D. *Anal. Bioanal. Chem*. **2007**, 387, 1235-1246.

6. Ning,B.; Graham, B.; Nigel, J. D.; and Lickiss, D. P. *J. Environ. Eng*. **2008**, 134, 944-954.

7. Meng, Z.; Chen,W.; and Mulchandani, A. *Environ. Sci. Technol*. **2005**, 39, 8958-8962.

8. Steger-Hartmann, T.; Langen, R.; Schweinfurth, H.; Tschampel M.; and Rehmann, I.; *Water Res.* **2002**, 36(1), 266-274.

9. Busetti, F.; Linge, K.; Blythe, J.; and Heitz, A. *J. Chromatagr. A*. **2008**, 1213(2), 200-208.

10. Putschew, A.; Schittko, S.; and Jekel, M. *J. Chromatogr. A*. **2001**, 930, 127-134.

11. Namasivayam, S.; Kalra K. M.; Torres, E.W.; and Small C. W. *Emerg. Radiol*. **2006**, 12, 210-215.

12. Desbrow, C.; Routledge, J. E.; Brighty, C.G.; Sumpter, J. P.; and Waldock, *Environ. Sci. Technol.* **1998**, 32, 1549–1558.

13. Zhurova, E. A.; Metta, F.C.; Wu, N.; Zhurov, V. V.; and Pinkerton, A. A. *J.Am. Chem. Soc.* **2006,** 128, 8849.

14. Tosha, T.; Kagawa, N.; Ohta, T.; Yoshioka, S.; Waterman, T. R., and Kitagwa, T. *Biochemistry*, **2006**, 45, 5631-5640.

15. Sieminska, L.; and Zerda, T.W. *J. Phys. Chem*. **1996**, 100, 4591.

16. Fan, Z.; Wu, S.; Chang, H.; and Hu. *J. Environ. Sci. Technol***. 2011**, 45, 2725–2733.

17. Joss, A.; Anderson, H.; Ternes, T.; Richle, R. P.; and Siergrist, H. *Environ. Sci. Technol*. **2004**, 38, 3047–3055.

18. Grover, D.P.; Zhanga, L. Z.; J.W. Readmanb, J.; and Zhoua, L. *Talanta,* **2009**, 78, 1204–1210.

19. Schafer, A. I.; Nghiem, L. D.; and Waite, T. D. *Environ. Sci. Technol*. **2003**, 37, 182-188.

20. Cartinella, A. L. J.; Cath, T.; Flynn, T. M.; Miller, C. G.; Hunter W. K.; JR.; and Childress. C. A. *Environ. Sci. Technl.* **2006**, 40, 7381-7386.

21. Wang, L.; Zhang, F.; Liu, R.; Zhang, Y. T.; Xue, X.; Xu, O.; and Liang, X. *Environ. Sci. Technol*. **2007**, 41, 3747-3751.

22. Seitz, W.; Weber, H. W.; Jiang J.Q.; Lloyd L. B.; Maier, D.; and Schulz, W. *Chemosphere*, **2006**, 64 (8), 1318–1324.

23. Munter, R. *Proc. Estonian Acad. Sci. Chem*. **2001**, 50, 59-80.

24. Gusseme, D. B.; Hennebal, T.; Vanhaecke, L.; Soetaert, M.; Desloover, J.; Wille, K.;Verbeken, K.; Verstraete, W.; and Boom, N. *Environ. Sci. Technol*. **2011**, 20, 5737-5745.

25. Tosha, T.; Kagawa, N.; Ohta, T.; Yoshioka, S.; Waterman, T. R.; and Kitagwa, T. *Biochemistry,* **2006**, 45, 5631-5640.

26. Kudo, A.; and Miseki, Y. *Chem. Soc. Rev*.**2009**, 38, 253-278

27. Busetti, F.; Linge, K.; Blythe, J.; and Heitz, A. *J. Chromatagr., A*. **2008**, 1213, 200-208.

28. Yan-fen, F.; Ying-ping, H.; De-fu, L.; Yang, H.; Wei, G.; and Johnson, D.J. *Environ. Sci*.**2008**, 97–102.

29. Znad, H.; and Y. Kawase. *J. Mol. Catal. A-Chem*. **2009**, 55-62.

30. Stafford, U.; Gray, K.; and Prashat, K. *Heterogen. Chem. Rev*. **1996**, 3, 77-104.

31. Ahmed, S.; Rasul, M. G.; Martens, W. N.; Brown, R. and Hashib, M. A. *Desalin. Water Treat*. **2010**, 261, 3-18.

32. Adán, C.; A. Bahamonde, A.; Martı´nez-Arias, M.; Ferna´ndez-Garcı´a, L.A.; and Pe´rez-Estrada, S. M.; *Catal. Today*. **2007**, 79–85.

33. Ternes, T.A.; Stuber, J.; Herrmann, N.; McDowell, D.; Ried, A.; Kampmann, M., and Teiser, B. *Water Res*. **2003**, 37, 1976-1982.

34. Doll, T.E.; and Frimmel, F.H. *Water Res.* **2005**, 39, 403-411.

35. Engel, T.; and Reid, P. Physical Chemistry. 2nd ed. Prentice Hall, **2010**.

36. Ostlund, S. N.; and Szabo, A. Modern Quantium Chemistry. 2nd ed. New York: Dover, **1998**.

37. Skoog, A. D.; Holler, J. F.; and Crouch, R. S. Principles of Instrumental Analysis. 5th ed. Belmont, CA, **1998**.

38. Foresman, B.J.; and Frisch, A. Exploring Chemistry with electronic Structure Methods. 2nd ed. Gaussian. **1993**.

39. Gaussian 09, Revision A.1, M. J. Frisch, G. W. Trucks, H. B. Schlegel, G. E. Scuseria, M. A. Robb, J. R. Cheeseman, G. Scalmani, V. Barone, B. Mennucci, G. A. Petersson, H. Nakatsuji, M. Caricato, X. Li, H. P. Hratchian, A. F. Izmaylov, J. Bloino, G. Zheng, J. L. Sonnenberg, M. Hada, M. Ehara, K. Toyota, R. Fukuda, J. Hasegawa, M. Ishida, T. Nakajima, Y. Honda, O. Kitao, H. Nakai, T. Vreven, J. A. Montgomery, Jr., J. E. Peralta, F. Ogliaro, M. Bearpark, J. J. Heyd, E. Brothers, K. N. Kudin, V. N. Staroverov, R. Kobayashi, J. Normand, K. Raghavachari, A. Rendell, J. C. Burant, S. S. Iyengar, J. Tomasi, M. Cossi, N. Rega, J. M. Millam, M. Klene, J. E. Knox, J. B. Cross, V. Bakken, C. Adamo, J. Jaramillo, R. Gomperts, R. E. Stratmann, O. Yazyev, A. J. Austin, R. Cammi, C. Pomelli, J. W. Ochterski, R. L. Martin, K. Morokuma, V. G. Zakrzewski, G. A. Voth, P. Salvador, J. J. Dannenberg, S. Dapprich, A. D. Daniels, Ö. Farkas, J. B. Foresman, J. V. Ortiz, J. Cioslowski, and D. J. Fox, Gaussian, Inc., Wallingford CT, 2009.

40. Sabin, F.; Türk, T.; and Vogler, A. Z. *Wasser-Abwasser-Forsch,***1992**, 25 163-167.

41. Kormann, C.; Bahnemann, D. W.; and Hoffmann, M. R. *Environ. Sci. Technol*. **1991**, 25, 494-500.

42. Doll, T. E.; and Frimmel, F.H. *Chemosphere,* **2003**, 52, 1757-1769.

43. Jeong, J.; Jung, J.; Cooper, W.J. and Song, W. *Water Res.* **2010**, 44, 4391-4398.

44. Hu, L.; Flanders, P.M.; Miller, P.L.; and Strathmann, T.J.; *Water Res.* **2007**, 41, 2612-2626.

45. Kormos, L. J.; Schulz, M.; Kohler, P., H., and Ternes, A., T., *Environ. Sci. Technol*. **2010**, 44, 4998-5007.

46. Huber, M.M.; Canonica, S.; Park, G.-Y.; and von Gunten, U. *Environ. Sci. Technol*. **2003**, (37), 1016-1055.

47. Batt, A. L.; Kim, S.; and Aga, D. *Environ. Sci. Technol.* **2006**, 40 (23), 7367–7373.

48. Desbrow, C.; Routledge, J. E.; Brighty, C.G.; Sumpter, J. P., and Waldock. *Environ. Sci. Technol*. **1998**, 32, 1549–1558.

49. Zhong- Qun, T.; Red, B; and De-Yin, W. *J. Phys. Chem. B* **2002**, 106, 9463-9483.

50. Perassi, M. E.; Canali,R. L.; and Coronado, A. E. *J. Phys. Chem. C* **2009**, 113, 6315–6319.

51. Zuo,C.; and Jagodzinski, W. P., J. *Phys. Chem. B* **2005**, 109, 1788–1793.

52. Emory, S.R.; Haskins, W.E.; and Nie, S. *J. Am. Chem. Soc.* **1998**, 120, 8009-8010.

53. Kneipp, K.; Kneipp, H.; Itzkan, I.; Dasar, R.R.; and Feld, M.S. *Chem. Rev.* **1999**, *99*, 2957-2975.

54. Badwaik, V. D.; Bartonojo, J. J.; Evans, J. W.; Sahi, S. V.; Willis, C. B.;Dakshinamurthy,R. *Langmuir*, **2011**, 27, 5549-5554.